Effects of the quantum fluctuations on the nonlinear optical response of trans-polyacetylene to the static external electric field

Akira Takahashi
Department of Advanced Materials Science and Engineering, Faculty of Engineering, Yamaguchi University, Ube 755, Japan
(Received 27 December 1996)

The nonlinear optical response to the strong static external electric field is investigated by the quantum Monte Carlo method in the Pariser-Parr-Pople model for trans-polyacetylene. The external field drives the electronic and lattice structures from a neutral dimerized state, through a charge-density-wave-like structure and to a charged soliton pairlike structure as its magnitude is increased. The external field dependence of the molecular polarization is strongly correlated to the evolution of these two structures. The quantum fluctuations of electrons drastically change the polarizability and hyperpolarizabilities when the parameters appropriate for trans-polyacetylene are used. The quantum lattice fluctuations have only negligible effects on them in this model in contrast to the case of the Su-Schrieffer-Heeger model. [S0163-1829(97)02731-8]

I. INTRODUCTION

Conjugated polymers have large hyperpolarizabilities, and therefore they are good candidates for optical devices.[1,2] Furthermore, they exhibit many interesting properties of fundamental interest originating from their low dimensionality. These include strong correlation effects[3,4] and nonlinear elementary excitations such as a soliton or a polaron.[5] It has been shown that these properties are closely related to their nonlinear optics.[1,6] Thus, the nonlinear optics is also an important tool to investigate these problems of fundamental interest.

Therefore, many theoretical studies have been done on the nonlinear optics of conjugated polymers. Full configuration-interaction calculations have been applied to the nonlinear optics of short polyenes, and it has been shown that the electron-electron correlation is crucial for the nonlinear optical properties of them.[1,7,8] These exact calculations can be applied only to very small systems (up to 12 carbon atoms so far) in practice. However, conjugated polymers have characteristic lengths that are closely related to their optical processes [the separation of an electron-hole pair of an exciton[9] (typically 40 carbon atoms) and the size of a soliton (about 14 carbon atoms)],[5] and it is essential to consider the system larger than these lengths to study the nonlinear optics of conjugated polymers.

Several authors have studied this problem by using the single configuration-interaction approximation,[10–12] which can be carried out for systems larger than these lengths. However, it is valid only when correlation effects are weak, and this is not the case for conjugated polymers. By the double configuration-interaction[13,14] or the time-dependent Hartree-Fock approximation,[15,16] more correlation effects can be taken into account. However, these methods still may not be enough to take account of the large correlation effects of conjugated polymers.

On the other hand, Hagler and Heeger proposed that the magnitudes of second hyperpolarizabilities are significantly enhanced by the quantum lattice fluctuations of soliton pairs,[6] and this was confirmed by the quantum Monte Carlo (QMC) study.[17] These studies have been done using the Su-Schrieffer-Heeger (SSH) model. However, since the Coulomb interaction, which is considered to be crucial for the optics of conjugated polymers, is neglected in the SSH model, it is not still clear whether this enhancement occurs or not in the model including the Coulomb interaction.

Considering these points, we study the nonlinear optical response to the static electric field in trans-polyacetylene, which is the simplest conjugated polymer, by the QMC method developed by Hirsch *et al.*[18] By using this method, we can overcome the difficulties mentioned above; large and nonlinear correlation effects and the quantum lattice fluctuations can be taken into account simultaneously by this method, and this method can be applied in practice to systems larger than the characteristic lengths mentioned above. Furthermore, the present method is not based on the conventional energy space picture but calculates real space physical quantities such as the charge density (CD) distribution induced by the external field. Therefore, it offers an obvious relation between the chemical structure and the optical properties, for example, how elementary excitations such as solitons affect the optical response.[16,19]

Conjugated polymers with donor and acceptor substitutions often show large hyperpolarizabilities and many experimental and theoretical studies have been done on how to maximize hyperpolarizabilities by designing the substitutions properly.[20–25] It has been shown that the static electric field produced by donor and acceptor changes their electronic and lattice structures and hyperpolarizabilities are enhanced by this structural change. Therefore, this problem is closely related to the problem considered in this paper. Moreover, since the correlation effects and the effects of lattice distortion are important also in donor and acceptor substituted conjugated polymers, the approach used in this paper will be very powerful also to this problem.

II. MODEL

We adopted the Pariser-Parr-Pople (PPP) Hamiltonian for a linear trans-polyacetylene chain interacting with a static electric field. The Hamiltonian is given by

$$H=H_{\mathrm{SSH}}+H_{\mathrm{C}}+H_{\mathrm{ext}}. \tag{1}$$

The first term H_{SSH} is the SSH Hamiltonian and is given by

$$H_{\mathrm{SSH}}=\sum_{n,m,\sigma} t_{m,n}\rho^{\sigma}_{n,m}+\frac{K}{2}\sum_{n}\ (u_{n+1}-u_n-\overline{y})^2+\frac{1}{2M}\sum_{n}\ p_n^2, \tag{2}$$

where K is the σ-bond spring constant, u_n is the displacement operator of the nth CH group along the chain direction, $\overline{y}$ is a constant that determines the mean bond length, M is the mass of the CH group, and p_n is the momentum operator conjugate to u_n. The π-electron density operators $\rho^{\sigma}_{n,m}$ are defined by

$$\rho^{\sigma}_{n,m}=c^{\dagger}_{m,\sigma}c_{n,\sigma}, \tag{3}$$

where the operator $c_{n,\sigma}$ ($c^{\dagger}_{n,\sigma}$) annihilates (creates) a π electron of spin σ at the nth site. $t_{n,n}$ is the Coulomb integral at the nth site and $t_{m,n}$ ($n\neq m$) is the transfer integral between the nth and mth sites. We considered hopping between only the nearest-neighbor sites. Thus,

$$t_{n,n}=-\sum_{m}\ V_{n,m}, \tag{4}$$

$$t_{n,n+1}=t_{n+1,n}=\overline{\beta}-\beta'(u_n-u_{n+1}), \tag{5}$$

and $t_{m,n}=0$ otherwise, where $V_{n,m}$ is a Coulomb repulsion between the nth and mth sites, $\overline{\beta}$ is the mean transfer integral between neighboring sites, and β' is the electron-phonon coupling constant.

The second term H_{C} represents the Coulomb interaction between π electrons and is given by

$$H_{\mathrm{C}}=\sum_{n}\ U\rho^{\uparrow}_{n,n}\rho^{\downarrow}_{n,n}+\sum_{n,m,\sigma,\sigma'}^{n\neq m} V_{n,m}\rho^{\sigma}_{n,n}\rho^{\sigma'}_{m,m}. \tag{6}$$

An on-site repulsion U is given by

$$U=\frac{U_0}{\varepsilon}, \tag{7}$$

and $V_{n,m}$ is given by the modified Ohno formula[26]

$$V_{n,m}=\frac{U_0}{\varepsilon\sqrt{1+(r_{n,m}/a_0)^2}}\ \text{ for }\ |m-n|\leqslant 1,$$
$$V_{n,m}=\frac{U_0}{\varepsilon\sqrt{1+(r_{n,m}/a_0)^2}}\exp(-\eta r_{n,m})\ \text{ for }\ |m-n|>1, \tag{8}$$

where $U_0=11.13$ eV is the unscreened on-site repulsion, $r_{n,m}$ is the distance between the nth and mth sites, and $a_0=1.2935$ Å. Note that there are two screening parameters in the formula: the dielectric constant ε and the screening constant of long-range part η.

The third term H_{ext} represents the interaction between the π electrons and the external static electric field E. Since the QMC method is applicable only to the static systems, we focus on the off-resonant nonlinear optics at zero frequency in this paper. The electric field is assumed to be polarized along the chain direction z. Within the dipole approximation, we then have

$$H_{\mathrm{ext}}=-EP, \tag{9}$$

where P is the molecular polarization operator

$$P=-e\sum_{n,\sigma}\ z(n)(\rho^{\sigma}_{n,n}-0.5), \tag{10}$$

where $-e$ is the electron charge and $z(n)$ is the z coordinate of the nth site.

In all the calculations in this paper, the system size was taken to be 40. We used the following parameters, which have been shown to be appropriate for trans-polyacetylene by previous works:[26] $\overline{\beta}=-2.38$ eV, $\beta'=2.99$ eV Å^{-1}, $K=40.2$ eV Å^{-2}, and $M=3145$ eV^{-1} Å^{-2}. The distances $r_{n,m}$ were calculated assuming a zigzag structure with a uniform bond length of 1.4 Å. We determined $\overline{y}$ as described in Ref. 27 to minimize the boundary effects; $\overline{y}=0.0968$ Å. As for the Coulomb screening parameters, Fukutome and coworkers have shown that many experiments can be explained by a single set of the parameters within the Hartree-Fock (HF) approximation; $\varepsilon=2$ and $\eta=0.38$ Å^{-1}.[26] However, since their studies are based on the HF approximation, which is not valid in the present case, ambiguities still exist in choosing them. Thus, we adopted not only Fukutome's screening parameters but also the other ones and studied the screening parameter dependence of nonlinear optical properties.

The expectation values of various physical quantities were calculated by the QMC method. The inverse of the temperature T^{-1} was taken to be 40 eV^{-1}. Since $\omega_0/T=4$, where $\omega_0=\sqrt{4K/M}$ is the bare optical phonon frequency, the effects of thermal phonon excitations are negligible. The Trotter number for electrons and that for phonons were taken to be 1200 and 40, respectively. To check the validity of these values, we calculated the ground-state energies of the coupled harmonic oscillators and the Hubbard model, which can be solved exactly, by the QMC method using these values. We compared the energies obtained by the present method with those of the exact solutions and found that the errors in them were both within a few percent.

To compare with the QMC results, we also calculated the same physical quantities by using the classical lattice and the HF approximations. In the classical lattice approximation, only lattice degrees of freedom were treated classically by taking the Trotter number for phonons to be 1 in the QMC simulation. In the HF approximation, the lattice coordinates were treated classically and the electronic and lattice structures were self-consistently determined so as to satisfy Hellmann-Feynman force equilibrium.

For convenience in the following, we here introduce two important physical quantities: the CD and the lattice order parameter (LOP). The CD at the nth site is given by

$$d_n=1-\sum_{\sigma}\ \langle\rho^{\sigma}_{n,n}\rangle, \tag{11}$$

where $\langle O\rangle$ indicates the expectation value of an operator O. The deviation of the bond length from the mean bond length at the nth bond is given by

$$y_n=\langle u_{n+1}\rangle-\langle u_n\rangle. \tag{12}$$

These quantities are decomposed into nonalternating and alternating components as

$$d_n=\overline{d_n}+(-1)^n d_n',$$

$$y_n=\overline{y_n}+(-1)^n y_n', \tag{13}$$

where the nonalternating and the alternating components are represented by an overbar and a prime, respectively. The operational definition of $\overline{d_n}$ is

$$\overline{d_n}=\tfrac{1}{4}(d_{n-1}+2d_n+d_{n+1}), \tag{14}$$

and the same formulas can be used for $\overline{y_n}$.[28] The LOP at the nth bond is defined by y_n', namely, the alternating component of the deviation of the bond length. Hence the LOP shows the strength of bond length alternation including the phase of the alternation. A bond-order wave state, where the bond length alternates uniformly, is characterized by the uniform and finite LOP and a charge density wave (CDW) state is also characterized by the uniform and finite d_n'. The expectation value of the molecular polarization operator $\langle P\rangle$ is determined by the CD distribution; it is derived from Eqs. (10) and (11) as

$$\langle P\rangle=e\sum_n z(n)d_n. \tag{15}$$

III. RESULTS BY THE HARTREE-FOCK APPROXIMATION

We calculated the E dependence of $\langle P\rangle$ by the HF approximation using the following Coulomb screening parameters: $\varepsilon=1$ and $\eta=0$, $\varepsilon=2$ and $\eta=0$, $\varepsilon=2$ and $\eta=0.38$ Å^{-1}, $\varepsilon=4$ and $\eta=0$, and $\varepsilon=4$ and $\eta=0.38$ Å^{-1}. We show them in Fig. 1. As seen from Fig. 1, they are classified into two types; in a type I (II), $\langle P\rangle$ is a concave (convex) function of E in the weak E range. The E dependence of $\langle P\rangle$ when $\varepsilon=2$ and $\eta=0.38$ Å^{-1} belongs to type I and the other ones belong to type II. In the following, we mainly focus on the following two sets of screening parameters, which belong to the different types: $\varepsilon=2$ and $\eta=0.38$ Å^{-1}, and $\varepsilon=2$ and $\eta=0$. The former set is chosen because it is the appropriate one for trans-polyacetylene and also because it is the only set that belongs to type I. The latter one is chosen as a typical case that belongs to type II. The results when the latter set is used qualitatively hold when the other sets that belong to type II are used.

We calculated polarizability (α) and second hyperpolarizability (γ) by fitting a curve

$$\langle P\rangle=\alpha E+\frac{1}{3!}\gamma E^3+\cdots \tag{16}$$

to the data using the least-squares method. Note that first hyperpolarizability $\beta=0$ because of the symmetry of the present Hamiltonian. We used the data in the range where the contribution to $\langle P\rangle$ from the third-order term to E is not negligible and it is much larger than those from the terms higher than third order; $0\leqslant E\leqslant 0.003$ V/Å when $\varepsilon=2$ and $\eta=0.38$ Å^{-1} and $0\leqslant E\leqslant 0.04$ V/Å when $\varepsilon=2$ and $\eta=0$. We took the terms up to seventh order in Eq. (16). Compared with the case when we take the terms up to fifth order, the difference in α is about 0.03% and the difference in γ is about 2%.

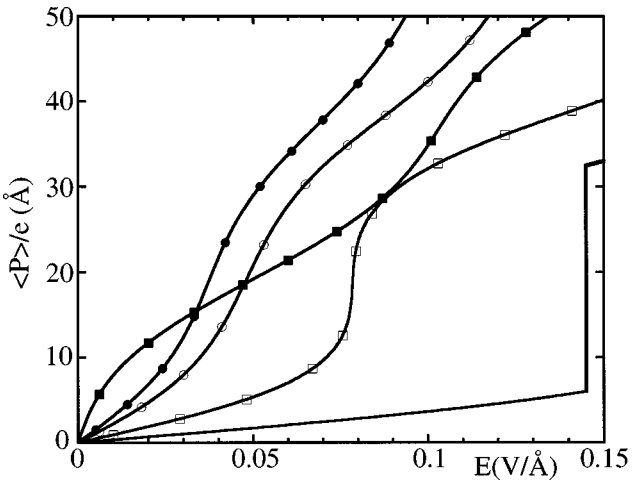

FIG. 1. The E dependences of $\langle P\rangle$ within the HF approximation. Those when $\varepsilon=1$ and $\eta=0$, when $\varepsilon=2$ and $\eta=0$, when $\varepsilon=2$ and $\eta=0.38$ Å^{-1}, when $\varepsilon=4$ and $\eta=0$, and when $\varepsilon=4$ and $\eta=0.38$ Å^{-1}, are shown by the solid line, the solid line with the open squares, the solid line with the closed squares, the solid line with the open circles, and the solid line with the closed circles, respectively.

We first show the results when $\varepsilon=2$ and $\eta=0.38$ Å^{-1}. Up to $E=0.002$ V/Å, $\langle P\rangle$ increases almost linearly to E. The slope $d\langle P\rangle/dE$ decreases with increasing E for $E<0.04$ V/Å; it is almost constant to E for 0.04 V/Å$<E<$0.06 V/Å, and it increases with increasing E for 0.06 V/Å$<E<$0.1 V/Å. To understand this characteristic E dependence of $\langle P\rangle$, we analyzed the CD and LOP distributions of the HF ground state at finite E. We show those for $E\leqslant 0.04$ V/Å in Fig. 2. There is no CD and LOP is almost uniform except for the chain edge regions when $E=0$. For $0<E<0.04$ V/Å, the CDW-like electronic structure is induced by E as seen from Fig. 2(a). This agrees with previous studies.[16,17] The magnitude of the CD of this structure increases with increasing E but the spatial CD distribution of this structure is almost unchanged to E in this range. Thus, we can approximately write the CD distribution in this range as

$$d_n(E)\cong A(E)d_n(E_0), \tag{17}$$

where E_0 is a certain external field in this range, and the amplitude $A(E)>0$ depends only on E. From Eqs. (15) and (17), we obtain $\langle P\rangle$ at E as

$$\langle P\rangle(E)\cong A(E)\langle P\rangle(E_0). \tag{18}$$

Therefore, the increase in $\langle P\rangle$ with increasing E is due to the growth of the CDW-like electronic structure in this range. For $E<0.002$ V/Å, $A(E)$ and therefore $\langle P\rangle$ increase almost

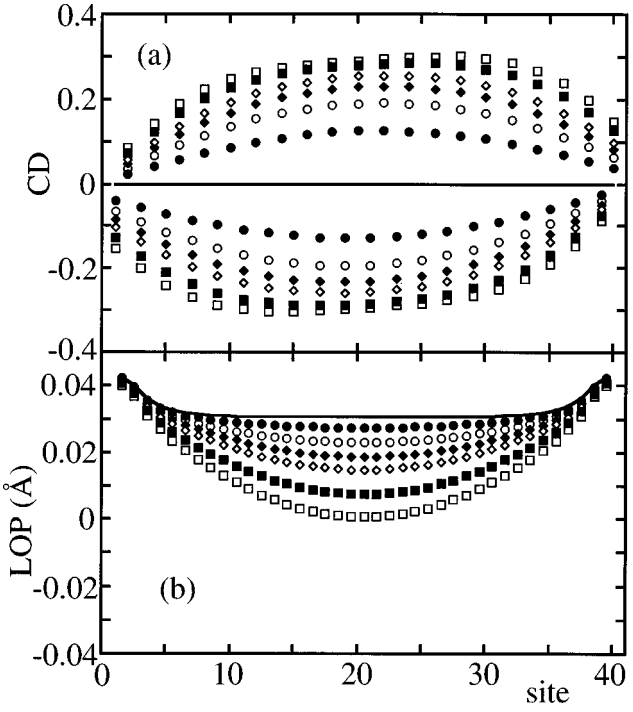

FIG. 2. (a) The CD and (b) LOP distributions of the ground state obtained by the HF approximation when $\varepsilon=2$ and $\eta=0.38$ Å^{-1}. Those at $E=0$, 0.005, 0.01, 0.015, 0.02, 0.03, and at 0.04 V/Å are shown by solid lines, closed circles, open circles, closed diamonds, open diamonds, closed squares, and open squares, respectively.

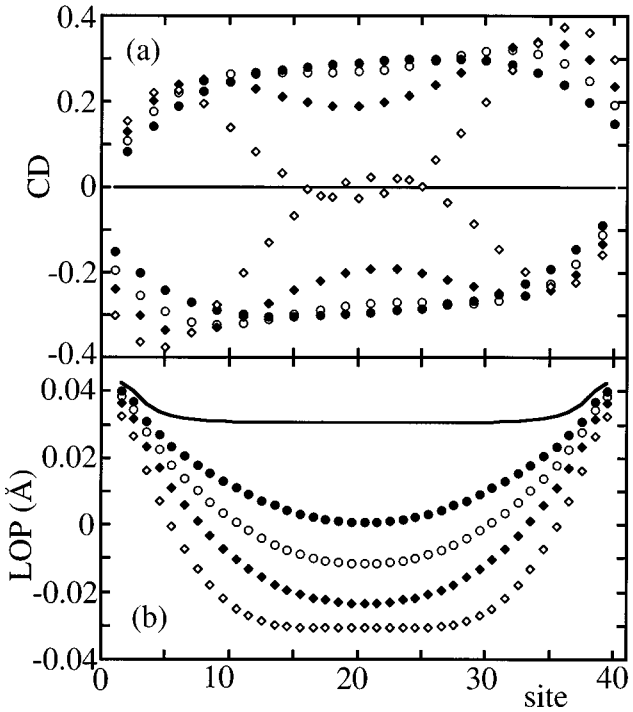

FIG. 3. (a) The CD and (b) LOP distributions of the ground state obtained by the HF approximation when $\varepsilon=2$ and $\eta=0.38$ Å^{-1}. Those at $E=0$, 0.04, 0.06, 0.08, 0.1 V/Å are shown by solid lines, closed circles, open circles, closed diamonds, and open diamonds, respectively.

linearly to E. For 0.002 V/Å$<E<$0.04 V/Å, $dA(E)/dE$ decreases with increasing E as seen from Fig. 2(a). As a result, $d\langle P\rangle/dE$ decreases with increasing E in this range.

We show the CD and LOP distributions of the HF ground state for 0.04 V/Å$\leqslant E\leqslant$0.1 V/Å in Fig. 3. Around $E=0.04$ V/Å, the magnitude of the CD of the CDW-like structure saturates and reaches the maximum value, which is almost the same as that of the metastable CDW HF solution when $E=0$. Above $E=0.04$ V/Å, the spatial CD distribution induced by E begins to change to E as seen from Fig. 3(a); the magnitudes of the CD decrease around the chain center and increase around the chain edges with increasing E. Furthermore, LOP's around the chain center decrease with increasing E and become negative above $E=0.06$ V/Å as seen from Fig. 3(b). Around $E=0.1$ V/Å, the characteristic electronic and lattice structures of a charged soliton pair with opposite net charges can be seen; the sign of LOP is reversed at the two soliton centers and there are two alternating CD clouds around there.[5,29] The CDW-like structure changes to the charged soliton pairlike structure as E is increased in the range $0.04<E<0.1$ V/Å. Since a charged soliton has net charge of $\pm e$, the charged soliton pairlike structure has large $\langle P\rangle$. The increase in $\langle P\rangle$ in this range is, therefore, attributed to the growth of the charged soliton pairlike structure. For $0.08<E<0.1$ V/Å, the structure grows most rapidly as seen from Fig. 3. Therefore, $\langle P\rangle$ increases rapidly there.

Above $E=0.1$ V/Å, a bipolaron pairlike structure grows, which causes the increase in $\langle P\rangle$ in this range.

We next show the results when $\varepsilon=2$ and $\eta=0$. The E dependence of $\langle P\rangle$ in this case differs so much from that when $\varepsilon=2$ and $\eta=0.38$ Å^{-1} as seen from Fig. 1. First, $\langle P\rangle$ is much smaller than that when $\varepsilon=2$ and $\eta=0.38$ Å^{-1} below $E=0.06$ V/Å. As a result, polarizability is reduced so much by the screening of the long-range Coulomb interaction; $\alpha(\eta=0.38)/\alpha(\eta=0)=12.8$. Second, $\langle P\rangle$ increases almost linearly to E up to $E=0.04$ V/Å in this case, and this value is about 20 times as large as the corresponding value when $\varepsilon=2$ and $\eta=0.38$ Å^{-1}. These differences can be understood in the following way. Up to $E=0.04$ V/Å, the CDW-like electronic structure is induced by E and the spatial CD distribution of this structure is almost unchanged to E also in this case. Therefore, the increase in $\langle P\rangle$ with increasing E is due to the growth of the CDW-like electronic structure in this range also in this case. The magnitude of the CD of the CDW-like electronic structure is, however, much smaller than that when $\varepsilon=2$ and $\eta=0.38$ Å^{-1} with the same E as seen by comparing Fig. 3(a) and Fig. 4(a). This is because the CDW-like structure is significantly stabilized by the screening of the long-range part of the Coulomb interaction.[29,30] As a result, $\langle P\rangle$ is much smaller than that when $\varepsilon=2$ and $\eta=0.38$ Å^{-1} in this case. Furthermore, since the magnitude is much smaller, it does not saturate and $\langle P\rangle$ increases almost linearly to E up to $E=0.04$ V/Å.

The slope $d\langle P\rangle/dE$ increases with increasing E above $E=0.04$ V/Å, shows very large peak around $E=0.08$ V/Å, and becomes small again around $E=0.1$ V/Å as seen from Fig. 1. We show the CD and LOP distributions for 0.06 V/Å $\leqslant E\leqslant$0.1 V/Å in Fig. 4. As seen from Fig. 4, the charged soliton pairlike structure begins to grow around $E=0.06$ V/Å, grows most rapidly around $E=0.08$ V/Å, and is almost completed around $E=0.1$ V/Å. Therefore, the characteristic rapid increase in $\langle P\rangle$ in this range can be attributed to the growth of this structure.

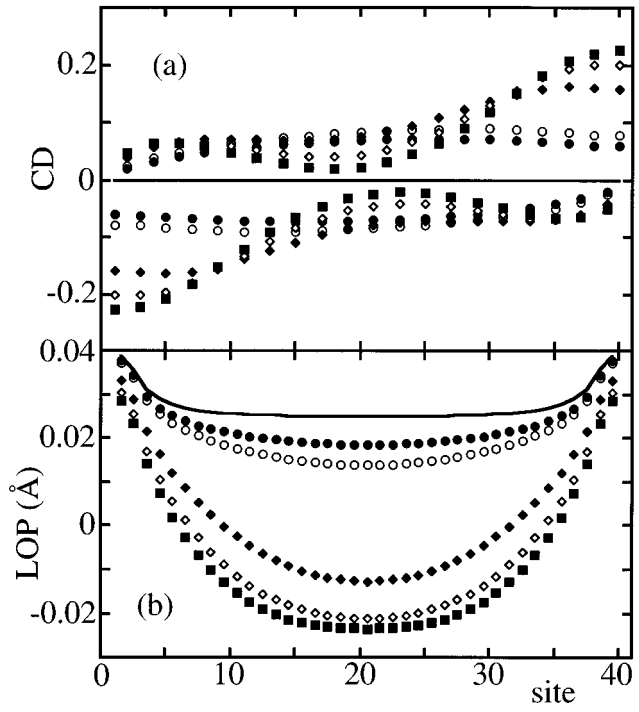

FIG. 4. (a) The CD and (b) LOP distributions of the ground state obtained by the HF approximation when $\varepsilon=2$ and $\eta=0$. Those at $E=0$, 0.06, 0.07, 0.08, 0.09, and 0.1 V/Å are shown by the solid lines, closed circles, open circles, closed diamonds, open diamonds, and closed squares, respectively.

When we use the unscreened Ohno potential ($\varepsilon=1$ and $\eta=0$), and also in the SSH model,[17] $\langle P\rangle$ of the HF ground state increases discontinuously to E at a certain external field E_c. In other words, there are CDW and charged soliton pair ''phases,'' and the first-order ''phase transition'' between these phases occurs at E_c. This characteristic behavior can be understood in the following way. When $\varepsilon=2$ and $\eta=0.38$ Å^{-1}, the CDW-like CD cloud in the weak external field range splits into two parts, and each part grows continuously into a charged soliton, which has an alternating CD cloud around the soliton center, as E is increased as seen from Fig. 3; there are stable intermediate states that connect the CDW and the charged soliton pair states in this case. However, when we use the unscreened Ohno potential or in the SSH model, the magnitude of the CD of the CDW-like electronic structure just below E_c is much smaller than that around the soliton center of a charged soliton. Therefore, there are no stable intermediate states that connect these two phases in these two cases, and a first-order phase transition between them occurs. When $\varepsilon=2$ and $\eta=0$, the magnitude of the CD of the CDW-like electronic structure is also much smaller than that of a charged soliton as seen from Fig. 4(a) but the difference is not so large compared with the cases where the discontinuous increase in $\langle P\rangle$ occurs. Thus, the CDW-like structure changes to a charged soliton pairlike structure very rapidly but continuously, which results in the characteristic rapid but continuous increase in $\langle P\rangle$ around $E=0.08$ V/Å in this case.

With all the sets of screening parameters that we have studied, E drives the electronic and lattice structures of the HF ground state from the neutral dimerized state, through the CDW-like structure, and to the charged soliton pairlike structure as E is increased. The evolution of these structures is strongly correlated to the E dependence of $\langle P\rangle$. In spite of the facts, the E dependences of $\langle P\rangle$ with the different Coulomb screening parameters differ very much. For example, in the two cases considered here, the sign of γ is reversed by introducing the screening of the long-range Coulomb interaction; $\gamma=-1.0\times10^{-26}$ esu when $\varepsilon=2$ and $\eta=0.38$ Å^{-1}, and $\gamma=3.3\times10^{-30}$ esu when $\varepsilon=2$ and $\eta=0$. When $\varepsilon=2$ and $\eta=0.38$ Å^{-1}, $dA(E)/dE$, and therefore $d\langle P\rangle/dE$, decrease as E is increased in the weak E range as shown above. Thus negative γ can be attributed to the slowdown of the growth of the CDW-like structure. On the other hand, when $\varepsilon=2$ and $\eta=0$, the soliton pairlike structure begins to grow before the growth of the CDW-like structure becomes slow, and $d\langle P\rangle/dE$ increases with increasing E in the weak E range. Therefore, positive γ in this case can be attributed to the growth of the soliton pairlike structure. The origins of optical nonlinearity differ between these two cases with the different screening parameters. The nonlinear optics is very sensitive to the Coulomb screening parameters within the HF approximation.

IV. RESULTS BY THE QUANTUM MONTE CARLO CALCULATIONS

We show the results by the QMC calculations in this section. In the QMC calculations, the quantum fluctuations of both the lattice and electrons are taken into account. To distinguish the effects of these two quantum fluctuations, we have also adopted the classical lattice approximation, where only the quantum fluctuations of electrons are taken into account. We found that the differences between the results by the QMC method and those by the classical lattice approximation are almost negligible in all the cases considered here. This shows that the effects of quantum fluctuations of the lattice on $\langle P\rangle$ are very small in the PPP model with the parameters considered in this paper. This result is in contrast to that obtained in the SSH model, where γ is significantly enhanced by the quantum fluctuations of the lattice.[6,17]

We first show the results when $\varepsilon=2$ and $\eta=0.38$ Å^{-1}. The quantum E dependence of $\langle P\rangle$ is compared with that of the HF case in Fig. 5. We calculated α and γ in the same way as the HF case using the data in the range $0\leqslant E\leqslant0.04$ V/Å. Since we do not have enough data and each datum contains statistical error, we took the terms up to the third order to E in Eq. (16) assuming that the contributions of the higher terms are not so large. The regression curve is also shown in Fig. 5. The data in the range are nicely fitted by the curve. However, when we take the terms up to fifth (seventh) order, α is altered by 5 (0.5)% and γ is altered by about 50 (50)%. Thus, we cannot obtain quantitative precision in γ by the present method.

By introducing the quantum fluctuations of electrons, the E dependence of $\langle P\rangle$ is drastically changed as seen from Fig. 5. The molecular polarization $\langle P\rangle$ increases almost linearly to E up to $E=0.02$ V/Å, and this value is 10 times as large as the corresponding value of the HF case with the same screening parameters. Furthermore, $\langle P\rangle$ and therefore α are significantly reduced by the quantum fluctuations in this range; $\alpha(\mathrm{QMC})/\alpha(\mathrm{HF})=0.16$. For 0.02 V/Å$<E<0.05$ V/Å, $d\langle P\rangle/dE$ increases with increasing E. As a result, γ is posi-

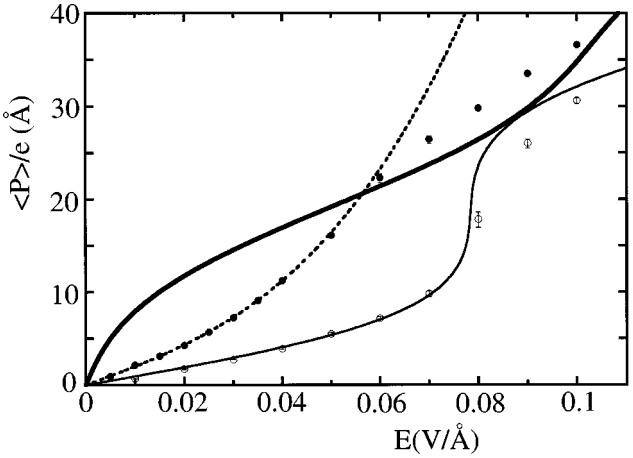

FIG. 5. The E dependence of $\langle P \rangle$ within the HF approximation when $\varepsilon=2$ and $\eta=0$, and that when $\varepsilon=2$ and $\eta=0.38$ Å^{-1} are shown by the thin and thick solid lines, respectively. The E dependence of $\langle P \rangle$ obtained by the QMC method when $\varepsilon=2$ and $\eta=0$, and that when $\varepsilon=2$ and $\eta=0.38$ Å^{-1}, are shown by the open and closed circles, respectively. The QMC samples are divided into five blocks. $\langle P \rangle$ for each part is calculated and their variances are shown as the error bars. The regression curve for the QMC results when $\varepsilon=2$ and $\eta=0.38$ Å^{-1} is shown by the dotted line.

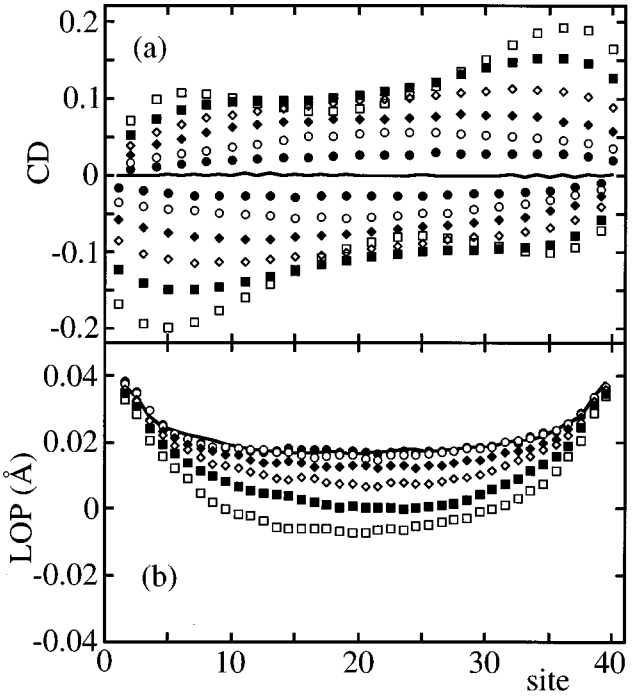

FIG. 6. (a) The CD and (b) LOP distributions of the ground state obtained by the QMC method when $\varepsilon=2$ and $\eta=0.38$ Å^{-1}. Those at $E=0$, 0.01, 0.02, 0.03, 0.04, 0.05, and 0.06 V/Å are shown by the solid lines, closed circles, open circles, closed diamonds, open diamonds, closed squares, and open squares, respectively.

tive in the QMC case ($\gamma=4.1\times10^{-29}$ esu); the sign of γ is reversed by introducing the quantum fluctuations of electrons. Above $E=0.06$ V/Å, $\langle P \rangle$ is enhanced by the quantum fluctuations contrary to their effects in the weak E range.

To understand these effects of the quantum fluctuations of electrons, we analyzed the CD and LOP distributions of the ground state at finite E. Those for $E\leqslant0.06$ V/Å are shown in Fig. 6. Below $E=0.02$ V/Å, where $\langle P \rangle \propto E$, the CDW-like electronic structure is induced also in the QMC case. However, the magnitude of the CD of this structure is much smaller than that of the HF case with the same E and screening parameters in this range as seen by comparing Fig. 2(a) and Fig. 6(a). This is the reason that $\langle P \rangle$ is reduced by the quantum fluctuations in this range. Similar effects of the quantum fluctuations are also observed in the QMC calculation of the charged soliton lattice ground state of doped polyacetylene; the magnitudes of the CD of the alternating CD cloud around the soliton centers are reduced significantly by them.[27] Moreover, since the magnitude of the CD of the CDW-like structure is much smaller in the QMC case, the range where the magnitude and therefore $\langle P \rangle$ increase almost linearly to E is much wider than that of the HF case with the same screening parameters.

As seen from Fig. 6, the charged soliton pairlike structure begins to grow with increasing E around $E=0.03$ V/Å; the CDW-like CD cloud splits into two parts and LOP's decrease around the chain center. The structure grows most rapidly around $E=0.05$ V/Å and the characteristic structure of a charged soliton pair is completed around $E=0.08$ V/Å. For $0.02<E<0.04$ V/Å, not only the soliton pairlike structure grows but also the magnitude of the CD of the CDW-like structure still increases as E is increased. Thus, the increase in $\langle P \rangle$ in this range is due to the growth of these two structures. The magnitude reaches a maximum value around 0.04 V/Å and the increase in $\langle P \rangle$ for $0.04<E<0.08$ V/Å is due to the growth of the charged soliton pairlike structure.

Since the charged soliton pairlike structure begins to grow before the growth of the CDW-like structure slows down, $d\langle P \rangle/dE$ increases with increasing E above $E=0.02$ V/Å and therefore γ is positive in the QMC case. Consequently, the origin of optical nonlinearity is altered by introducing the quantum fluctuations of electrons.

Although $\langle P \rangle$ is larger in the QMC case than in the HF case for $E\geqslant0.06$ V/Å, the magnitude of the CD induced by E is still smaller in the QMC case than in the HF case as seen by comparing Fig. 3(a) and Fig. 6(a). This may look inconsistent with the previous discussions but can be understood as follows. The CD is decomposed into the nonalternating and the alternating components as described in Sec. II. The magnitude of the alternating component is larger than that of the nonalternating one both in the CDW-like electronic structure and in the charged soliton pairlike structure with all the sets of parameters considered in this paper. In particular, the difference in magnitude between these two components is very large in the CDW-like structure. However, the nonalternating component has much larger contributions to $\langle P \rangle$ than the alternating one. In the CDW-like structure, both components are reduced in magnitude by the quantum fluctuations and the reduction is larger in the alternating one. In the charged soliton pairlike structure, the magnitude of the alternating component is reduced but that of the nonalternating one and therefore $\langle P \rangle$ are enhanced by the quantum fluctuations.

We next show the results when $\varepsilon=2$ and $\eta=0$. For $E<0.07$ V/Å, $\langle P \rangle$ is almost unchanged by introducing the quantum fluctuations of electrons as seen from Fig. 5. In this range, the CDW-like electronic structure is induced by E also in the QMC case. The alternating component of the CD

of this structure is reduced by the quantum fluctuations in magnitude but the nonalternating component is almost unchanged in this case. As a result, although the CD distribution is altered by the quantum fluctuations, $\langle P \rangle$ is almost unchanged by them in this range.

In the HF case, $\langle P \rangle$ increases abruptly at $E=0.08$ V/Å. By introducing quantum fluctuations, the sharp increase becomes more gradual. The ground states around $E=0.08$ V/Å can be regarded as the intermediate states that connect the two stable CDW and charged soliton pair states as mentioned in Sec. III. We can expect that such intermediate states are less stable and the magnitude of the quantum fluctuations is larger in them compared with the CDW and charged soliton pair states. This can be seen directly in the following way. We divided QMC samples into five blocks and calculated $\langle P \rangle$ for each part. Their variances are shown as the error bars in Fig. 5. The variance at $E=0.08$ V/Å is much larger than the other ones. This shows that the quantum fluctuations increase there in magnitude. Such large quantum fluctuations in the intermediate states make the sharp increase in $\langle P \rangle$ less steep.

The evolution of the CDW-like and charged soliton pairlike structures is strongly correlated to the E dependence of $\langle P \rangle$ also in these two QMC cases with the different screening parameters. However, the nonlinear optical response differs so much between the two cases with the different Coulomb screening parameters also in the QMC case. Therefore, we must be very careful in choosing them when we calculate nonlinear optical properties. Moreover, this result indicates that γ can be changed drastically if we can control the screening parameters.

V. DISCUSSIONS

Only the static electric field is considered in this paper, while experimental measurements have been done at finite frequencies.[1,2] Therefore, the present result cannot be compared directly with the experiments; the present study underestimates the contributions from those excited states whose excitation energies are near the frequency of the light used in the experiments. However, if the frequency is far enough from the resonant ones, the difference will not be so large.

In the previous studies, it has been shown that the quantum fluctuations of the lattice play an important role in the linear and nonlinear optics in the SSH model for trans-polyacetylene.[6,17] This result is in contrast to the present one, where the effects of quantum fluctuations of the lattice are negligible. The difference can be understood as follows. First, in the SSH model with the parameters appropriate for trans-polyacetylene, the electron-phonon coupling constant $\beta'=4.07$ eV/Å and this value is much larger than that in the PPP model. This is because some effects of the Coulomb interaction can be taken into account by increasing β'.[30] Thus, the effects of the quantum fluctuations of the lattice are overestimated in the SSH model. Second, in the SSH model, γ is enhanced mainly by the hybridization of the charged soliton pair state to the CDW-like classical ground state as a quantum fluctuation of the lattice.[17] In the present model, such hybridization occurs also as a result of the quantum fluctuations of electrons. Therefore, the effects of quantum fluctuations of the lattice are hidden by those of the large quantum fluctuations of electrons.

In donor and acceptor substituted trans-polyacetylene, the static electric field is produced by the charge of donor ($Q_D>0$) and the opposite charge of acceptor ($-Q_D$). Its electronic and lattice structures are changed by the electric field and hyperpolarizabilities are enhanced by this structural change.[20–22] Since this static electric field can be approximated roughly by the uniform static electric field considered here, we can approximately regard the effects of uniform static field as those of donor and acceptor substitutions. Then Q_D in donor and acceptor substituted trans-polyacetylene corresponds to E in the present problem. From the E dependence of $\langle P \rangle$, we can obtain α, β, and γ at E as

$$\alpha(E)=\frac{d\langle P(E)\rangle}{dE},$$

$$\beta(E)=\frac{d^2\langle P(E)\rangle}{dE^2}, \tag{19}$$

$$\gamma(E)=\frac{d^3\langle P(E)\rangle}{dE^3}.$$

They can be regarded as those of donor and acceptor substituted trans-polyacetylene with Q_D, which corresponds to E.

It has been shown that the changes in the lattice structure are strongly correlated to the polarizability and hyperpolarizabilities in donor and acceptor substituted short polyenes; as Q_D is increased, LOP's decrease at all the bonds and the sign of the average of LOP over all the bonds is reversed at a certain Q_D. The hyperpolarizabilities are significantly enhanced when the average of LOP becomes almost zero.[20–22] In the present case, the soliton pairlike lattice structure grows with increasing E and LOP's decrease only in the region between the solitons. The difference is attributed to the fact that the system size considered in the previous studies of donor and acceptor substituted polyenes was too small to describe the formation of a soliton pair. The changes in the lattice structure, that is, the growth of the charged soliton pairlike lattice structure, is strongly correlated to α, β, and γ also in the present case. In the HF case when $\varepsilon=2$ and $\eta=0$, $\langle P \rangle$ increases very rapidly around $E=0.08$ V/Å, where the charged soliton pairlike structure grows most rapidly, and E dependence of $\langle P \rangle$ shows a step-function-like behavior. As a result, α and $|\gamma|$ become the largest around $E=0.08$ V/Å and $|\beta|$ becomes the largest a little above or below there, and these maximum values are much larger than those when $E=0$. When the quantum fluctuations are taken into account, $d\langle P \rangle/dE$ around $E=0.08$ V/Å is reduced but it still shows a very sharp peak there. Thus, these maximum values of the polarizabilities are reduced by the quantum fluctuations but they are still much larger than those when $E=0$ also in the QMC case. Consequently, large hyperpolarizabilities can be expected by proper substitution of donor and acceptor when $\varepsilon=2$ and $\eta=0$.

In the QMC case when $\varepsilon=2$ and $\eta=0.38$ Å^{-1}, the step-function-like sharp increase is not seen in the E dependence of $\langle P \rangle$. Thus, hyperpolarizabilities become larger around $E=0.05$ V/Å, where $\langle P \rangle$ changes most rapidly, than those when $E=0$ but the enhancements are not so large. This in-

dicates that large hyperpolarizabilities will not be obtained by donor and acceptor substitution when we use these parameters. As seen from Fig. 1, as η or ε becomes smaller, namely, the screening of the Coulomb interaction becomes weaker, the step-function-like behavior in E dependence of $\langle P \rangle$ becomes sharper and larger hyperpolarizabilities will be obtained by substitution of proper donor and acceptor.

As long as uniform E is considered, only qualitative analysis is possible for donor and acceptor substituted transpolyacetylene. The QMC method used in this paper is applicable to this problem. This problem is a subject for a future study.

VI. SUMMARY

We studied the nonlinear optical response of transpolyacetylene to the static external electric field. The external field drives the electronic and lattice structures of transpolyacetylene from the neutral dimerized state, through the CDW-like structure and to the charged soliton pairlike structure as its magnitude is increased. The evolution of these two structures is strongly correlated to the E dependences of $\langle P \rangle$ with all the screening parameters considered in this paper both in the QMC and HF cases. The polarizability and hyperpolarizabilities are very sensitive to the Coulomb screening parameters. When the screening parameters appropriate for trans-polyacetylene ($\varepsilon=2$ and $\eta=0.38$ Å^{-1}) are used, the quantum fluctuations of electrons drastically change the linear and nonlinear optical response; α is decreased to 16% and the sign of γ is reversed by introducing them. When $\varepsilon=2$ and $\eta=0$, the quantum fluctuations of electrons have only negligible effects on $\langle P \rangle$ in the low E range but the characteristic sharp increase of $\langle P \rangle$ at $E=0.08$ V/Å become less steep by introducing them. The effects of quantum lattice fluctuations are negligible with both the sets of screening parameters in contrast to the case of the SSH model.

[1] S. Etemad and Z. G. Soos, in *Spectroscopy of Advanced Materials*, edited by R. J. H. Clark and R. E. Hester (Wiley, New York, 1991).

[2] J.-L. Brédas, C. Adant, P. Tackx, A. Persoons, and P. M. Pierce, Chem. Rev. **94**, 243 (1994).

[3] K. Schulten, I. Ohmine, and M. Karplus, J. Chem. Phys. **64**, 4422 (1976).

[4] I. Ohmine and M. Karplus, J. Chem. Phys. **68**, 2298 (1978).

[5] A. J. Heeger, S. Kivelson, J. R. Schrieffer, and W.-P. Su, Rev. Mod. Phys. **60**, 781 (1988), and references therein.

[6] T. W. Hagler and A. J. Heeger, Chem. Phys. Lett. **189**, 333 (1992); Phys. Rev. B **49**, 7313 (1994).

[7] S. N. Dixit, D. Guo, and S. Mazumdar, Phys. Rev. B **43**, 6781 (1991).

[8] S. Mazumdar, D. Guo, and S. N. Dixit, Synth. Met. **57**, 3881 (1993).

[9] H. X. Wang and S. Mukamel, J. Chem. Phys. **97**, 8019 (1992).

[10] S. Abe, M. Schreiber, and W.-P. Su, Chem. Phys. Lett. **192**, 425 (1992).

[11] S. Abe, M. Schreiber, W.-P. Su, and J. Yu, Phys. Rev. B **45**, 9432 (1992).

[12] D. Yaron and R. Silbey, Phys. Rev. B **45**, 11 655 (1992).

[13] J. R. Heflin, K. Y. Wong, O. Zamani-Khamiri, and A. F. Garito, Phys. Rev. B **38**, 1573 (1988); Mol. Cryst. Liq. Cryst. **160**, 37 (1988).

[14] V. A. Shakin and S. Abe, Phys. Rev. B **50**, 4306 (1994).

[15] H. Sekino and R. J. Bartlett, J. Chem. Phys. **85**, 976 (1986).

[16] A. Takahashi and S. Mukamel, J. Chem. Phys. **100**, 2366 (1994).

[17] A. Takahashi, Phys. Rev. B **51**, 16 479 (1995).

[18] J. E. Hirsch, R. L. Sugar, D. J. Scalapino, and R. Blankenbecler, Phys. Rev. B **26**, 5033 (1982).

[19] S. Mukamel, A. Takahashi, H. X. Wang, and G. Chen, Science **266**, 250 (1994).

[20] S. R. Marder, J. W. Perry, G. Bourhill, C. B. Gorman, B. G. Tiemann, and K. Mansour, Science **261**, 186 (1993).

[21] S. R. Marder, C. B. Gorman, F. Meyers, J. W. Perry, G. Bourhill, J.-L. Brédas, and P. M. Pierce, Science **265**, 632 (1994).

[22] G. Chen and S. Mukamel, J. Chem. Phys. **103**, 9355 (1995).

[23] Y. Matsuzaki, K. Tanaka, and T. Yamabe, Chem. Phys. Lett. **230**, 443 (1994).

[24] I. D. L. Albert, D. Pugh, and J. O. Morley, J. Chem. Soc. Faraday Trans. **90**, 2617 (1994).

[25] N. Matsuzawa and D. A. Dixon, J. Phys. Chem. **98**, 2545 (1994).

[26] H. Fukutome, J. Mol. Struct. **188**, 337 (1989), and references therein.

[27] A. Takahashi, Phys. Rev. B **54**, 7965 (1996).

[28] A. Takahashi and H. Fukutome, Solid State Commun. **62**, 279 (1987).

[29] H. Fukutome and M. Sasai, Prog. Theor. Phys. **69**, 373 (1983).

[30] H. Fukutome and M. Sasai, Prog. Theor. Phys. **69**, 1 (1983).